Separation Science and Technology
Publication details, including instructions for authors and subscription information:
http://www.informaworld.com/smpp/title~content=t713708471

Modeling of the Mass Transfer Rates of Metal Ions across Supported Liquid Membranes. II. Comparison between Theory and Experiment

A. A. Elhassadi; D. D. Do[a]
[a] DEPARTMENT OF CHEMICAL ENGIEERING, UNIVERSITY OF QUEENSLAND, ST. LUCIA, QUEENSLAND, AUSTRALIA

Online publication date: 22 February 1999

SEPARATION SCIENCE AND TECHNOLOGY, **34**(3), pp. 461–486, 1999

Modeling of the Mass Transfer Rates of Metal Ions across Supported Liquid Membranes. II. Comparison between Theory and Experiment

A. A. ELHASSADI*
DEPARTMENT OF CHEMISTRY
UNIVERSITY OF GARYOUNIS
BENGHAZI, LIBYA

D. D. DO
DEPARTMENT OF CHEMICAL ENGINEERING
UNIVERSITY OF QUEENSLAND
ST. LUCIA, QUEENSLAND 4067, AUSTRALIA

ABSTRACT

The model equations developed in Part I were tested using experimental data reported in the literature and produced in this work. It was found that uranium(VI) and thorium(IV) can be selectively separated and concentrated using supported liquid membranes. Depending on the way the liquid membranes are designed, the selectivity toward a specific metal can be predetermined. The effect of the ratio of the effective diffusivity to bulk diffusivity in free solution was found to behave with the same characteristic of systems of preferentially adsorbed solutes.

INTRODUCTION

This paper deals with the experimental determination and theoretical simulation of the intrinsic parameters that characterize design model equations describing the transport of metal ions across liquid membranes. A literature review of this vast area is not considered in this paper because it has been

* To whom correspondence should be addressed. Present address: c/o Ashref M. Dardi, 42-31 Centennial Street, Regina, SK S4S 6P8, Canada.

covered in detail in many earlier works [Kopp et al. (1), Marr and Kopp (2), Chan and Lee (3), Darbi (4), Hassan (5), and Elhassadi and Do (6)].

It is the intension of all research work to develop models that describe the behavior of a system quite accurately and precisely. Murthy and Gupta (7) tried to rearrange the solution–diffusion model and the film theory model in order to estimate membrane parameters, previously estimated using Kimura–Sourirajan analysis. Good results were obtained.

Zuo et al. (8) tried to apply the Danesi model to facilitated transport of gold through a three-compartment membrane system using similar membranes. The influences of the stirring rate in aqueous feed and organic solutions, of the stripping reagents and their concentration, of the carrier concentration, and of the concentration of HCl in the aqueous feed on the permeability coefficients were studied.

Wodzki and Sionkowski (9) examined the performance of a multimembrane hybrid system made up of ion-exchange membranes and a bulk liquid membrane. Fluxes and separation among Zn(II), Cu(II), Co(II), and Ni(II) sulfates were studied as dependent on the concentration of the aqueous phases and temperature. Selectivity coefficients calculated amount to 30–40. To diminish the number of variables, only experiments under quasi-steady-state conditions were carried out.

Kondo and Matsumoto (10) studied the extraction and permeation of europium and found them to be limited by the diffusion and reaction resistances, respectively. They reported that an improvement of the separation factor under the condition of reaction control is easier than that under diffusion control. They utilized the eigenmechanism rule as follows: a) if the rate constant of the complex formation is large as it is for most metal ions, the extraction is limited by the diffusion process; b) in the case of a small rate constant, as for Fe(III), the rate is limited by the interfacial reaction. The separation factor was enhanced by utilizing the differences in the stability constants between the chelating reagent and lanthanides.

Vural (11) developed a similar Michaelis–Menton model to study the active transport properties of metal picrates by two new calixarene types. Maximum flux and extraction equilibrium constants were estimated using the suggested model. The results showed an excellent fit with a value of $l/\mathscr{D} = 1.7 \times 10^{-3}$ s·cm^{-1}, which corresponds to a diffusion layer thickness of around 500 μm for high diffusion coefficients ($\mathscr{D} = 10^{-4}$ cm^2·s^{-1}).

Interest has arisen in testing the durability of the membrane material in resisting heat, chemicals, corrosion, etc. influences of different media. Unfortunately, polymeric materials from which most commercial membranes are currently produced do not necessarily meet these requirements. For this reason we tried to apply our model on existing inorganic membranes data available in the literature because they possess similar mean pore radii with broader pore size

distributions compared to polymeric films. Available data for such a purpose are not mature because inorganic membrane applicability to membrane separation technology has not yet been fully developed (12). It is the purpose of this paper to enhance the development of modeling in this very important area of research. Previous trials have become stagnant at a certain level.

FLUX ANALYSIS

Single Systems

Theoretical development of facilitated diffusion has been restricted to cases that provide limits to the behavior of a facilitating carrier such as fast reaction and fast diffusion. Fick's law is applicable for diffusion within the membrane with the assumption that the diffusion coefficient is independent of concentration and spatial coordinates as follows:

$$J = -\mathscr{D}_e \frac{\partial C}{\partial x} \tag{1}$$

where $\mathscr{D}_e$ is the effective diffusivity defined in terms of the geometrical factors affecting the membrane network. Fick's law can be expressed in nondimensional form (6) as

$$J = -\frac{\mathscr{D}_e}{l} C_{b10} K_{e1} \frac{\partial E}{\partial y} \tag{2}$$

A simplifying assumption is imposed in this development. That is, a pseudosteady-state assumption of the concentration within the membrane prevails. In this article we look at flux development of the least restricted case and the most restricted case (6).

Fast Interfacial Reactions with Negligible Aqueous Diffusional Resistances

Using the concentration profiles obtained in Part I (6), Eq. (2) can be differentiated to give

$$J = \frac{\mathscr{D}_e}{l} C_{b10} K_{e1} (h - \beta g) = \frac{\mathscr{D}_e}{l} C_{b10} K_{e1} (1 - \beta\gamma) e^{-(1 + \frac{\alpha'}{\alpha}\beta)\tilde{t}} \tag{3}$$

Initially, the flux profile is a function of the chemical system as dictated by the simultaneous extraction–stripping process. The flux profile decays to negligible values after very long times, as expected. Depending on the mechanism involved and the carrier selection, that is, whether one uses a neutral extractant carrier or an acidic carrier, the carrier selected can cause fascinating effects such as cotransport or countertransport of the solute species and their coupling ion, respectively. For the case of divalent metals, K_{e1} and K_{e2} can be derived for chemical systems characterized by fast chemical reactions as

MARCEL DEKKER, INC.
270 Madison Avenue, New York, New York 10016

$$K_{e1} = \frac{(Ml_2 \cdot 2TBP)_{O1}}{(M^{2+})_{O1}} \frac{1}{(l^-)^2_{A1}\,(TBP)^2_{O1}} \quad (4a)$$

$$K_{e2} = \frac{(Ml_2 \cdot 2TBP)_{O2}}{(M^{2+})_{A1}} \frac{1}{(l^-)^2_{A2}\,(TBP)^2_{O2}} \quad (4b)$$

for a neutral extractant carrier (cotransport mechanism)

$$K_{e1} = \frac{[M(HG_2)_2]_{O1}}{(M^{2+})_{A1}} \frac{(H^+)^2_{A1}}{[(HG)_2]^2_{O1}} \quad (4c)$$

$$K_{e2} = \frac{[M(HG_2)_2]_{O2}}{(M^{2+})_{A2}} \frac{(H^+)^2_{A2}}{[(HG)_2]^2_{O2}} \quad (4d)$$

for an acidic extractant carrier (countertransport mechanism)

where the subscripts O and A refer to the organic and aqueous phases, respectively. H^+ and l^- refer to the coupling ion which represents the hydrogen ion in the case of the countertransport mechanism and the ligand ion in the case of the cotransport mechanism. HG and TBP represent the acidic extractant carrier and the neutral extractant carrier, respectively. K_e represents the effective equilibrium constant which is a function of the equilibrium constant of the heterogeneous reaction, the deviation of the concentration of each species in the chemical system from their respective activities, and the degree of formation of the different complexes of the solute species with the ligand in the aqueous phases.

Slow Interfacial Reactions with Aqueous Diffusional Resistances

Using the concentration profiles obtained in Part I (6), Eq. (2) can be differentiated to give

$$J = \frac{\mathcal{D}_e}{l} C_{b10} K_{e1} \left(\frac{1 - \beta\gamma}{\Omega} \right) e^{-\frac{1}{\Omega}(1 + \frac{\alpha'}{\alpha}\beta)\tilde{t}} \quad (5)$$

where $\Omega = 1 + K_{e1}(B_{i1}^{-1} + N_1^{-1}) + K_{e2}(B_{i2}^{-1} + N_2^{-1})$. This equation shows the role of aqueous mass transfer resistance and reaction-limited resistance in the extraction side and in the stripping side.

Binary Systems

For the competitive transport of a metal species M and another metal species N, the ratio of the two fluxes J_M and J_N can be written for the simple case of fast interfacial reactions with negligible aqueous diffusional resistance

MARCEL DEKKER, INC.
270 Madison Avenue, New York, New York 10016

as

$$\frac{J_{\mathrm{M}}}{J_{\mathrm{N}}} = \frac{\mathscr{D}_{\mathrm{e}}^{\mathrm{M}} C_{\mathrm{b10}} K_{\mathrm{e1}}^{\mathrm{M}} (h^{\mathrm{M}} - \beta^{\mathrm{M}} g^{\mathrm{M}})}{\mathscr{D}_{\mathrm{e}}^{\mathrm{N}} C_{\mathrm{b10}}^{\mathrm{N}} K_{\mathrm{e1}}^{\mathrm{N}} (h^{\mathrm{N}} - \beta^{\mathrm{N}} g^{\mathrm{N}})}$$

$$= \frac{\mathscr{D}_{\mathrm{e}}^{\mathrm{M}} C_{\mathrm{b10}}^{\mathrm{M}} K_{\mathrm{e1}}^{\mathrm{M}} (1 - \beta^{\mathrm{M}} \gamma^{\mathrm{M}}) \exp(-(1 + \left(\frac{\alpha'}{\alpha}\right)^{\mathrm{M}} \beta^{\mathrm{M}}) \tilde{t})}{\mathscr{D}_{\mathrm{e}}^{\mathrm{N}} C_{\mathrm{b10}}^{\mathrm{N}} K_{\mathrm{e1}}^{\mathrm{N}} (1 - \beta^{\mathrm{N}} \gamma^{\mathrm{N}}) \exp(-(1 + \left(\frac{\alpha'}{\alpha}\right)^{\mathrm{N}} \beta^{\mathrm{N}}) \tilde{t})} \quad (6)$$

Equations (3) and (6) can be simplified to account for some simple special cases, like that of Lee et al. (13) or Danesi et al. (14), by making use of the following assumptions: a) All solutes in the membrane have the same effective diffusivity; b) initially, the solute concentration in the stripping side is equal to 0 (i.e., $\gamma = 0$); and c) initially, when t is very close to 0, the term $[1 + (\alpha'/\alpha)\beta]\tilde{t}$ can be assumed to be negligible. With these simplifying assumptions, Eqs. (3) and (6) can be written as

$$J = \frac{\mathscr{D}_{\mathrm{e}}}{l} C_{\mathrm{b10}} K_{\mathrm{e1}} \quad (7)$$

$$\frac{J_{\mathrm{M}}}{J_{\mathrm{N}}} = \frac{C_{\mathrm{b10}} K_{\mathrm{e1}}^{\mathrm{M}}}{C_{\mathrm{b10}}^{\mathrm{N}} K_{\mathrm{e1}}^{\mathrm{N}}} \quad (8)$$

Using the definition of the permeability (i.e., $P = J/C_{\mathrm{b10}}$, the permeation rate extrapolated to time 0), Eqs. (7) and (8) become

$$P = \frac{J}{C_{\mathrm{b10}}} = \frac{\mathscr{D}_{\mathrm{e}}}{l} K_{\mathrm{e1}} \quad (9)$$

$$\frac{P_{\mathrm{M}}}{P_{\mathrm{N}}} = \frac{K_{\mathrm{e1}}^{\mathrm{M}}}{K_{\mathrm{e1}}^{\mathrm{N}}} \quad (10)$$

Equation (5) can also be simplified to account for some special cases, like that of Danesi et al. (14, 15), by making use of the following assumption: d) The rates of the chemical reactions and the rate of mass transfer within the boundary layer in the stripping side are assumed to be negligible. Then, one would obtain the following relation:

$$P = \frac{J}{C_{\mathrm{b10}}} = \frac{k_1}{1 + \frac{l}{\mathscr{D}_{\mathrm{e}}} k_{-1} + \frac{k_1}{k_{\mathrm{m1}}}} \quad (11)$$

where $l/\mathscr{D}_{\mathrm{e}} = \Delta_0$ and $K_{\mathrm{m1}}^{-1} = \Delta_{\mathrm{a}}$ in Danesi et al.'s (15) development. This gives rise to the three controlling regions: (a) Kinetically controlled region, where $1 + (l/\mathscr{D}_{\mathrm{e}})k_1 + (k_1/k_{\mathrm{m1}}) \approx 1$ and $P = k_1$; (b) membrane diffusion con-

trolled where $1 + (l/\mathscr{D}_e)k_1 + (k_1/k_{m1}) \approx (l/\mathscr{D}_e)k_1$ and $P = (\mathscr{D}_e/l)\,k_{e1}$, which is equal to Eq. (9); (c) aqueous boundary layer controlled where $1 + (l/\mathscr{D}_e) + (k_1/k_{m1}) \approx k_1/k_{m1}$ and $P = k_{m1}$.

When comparing Eqs. (5) and (6) with Eqs. (7) and (8), one finds that Eqs. (7) and (8) compare the fluxes in a dynamic sense (i.e., with respect to time) rather than in a thermodynamical equilibrium sense. This is very important in selective separations because it gives us an idea about the history of the concentration and selective separations and when it is best to stop the process.

Relationship between Equilibrium Constant and Distribution Coefficient

The steady-state metal–carrier flux can be represented by the simplified Fick's first law of diffusion as

$$J = \frac{\mathscr{D}_e}{l}[C(0,t) - C(l,t)] \tag{12}$$

When the experimental conditions are such that $C(l,t) \ll C(0,t)$, and considering that $D_1 = C(0,t)/C_{b1}$, then

$$J = \frac{\mathscr{D}_e}{l} C_{b1} D_1 \tag{13}$$

Using the definition of permeability coefficient, $P = J/C_{b1}$, gives

$$P = \frac{\mathscr{D}_e}{l} D_1 \tag{14}$$

Another way of looking at this is by solving the governing equations of the fast interfacial reactions with the negligible aqueous diffusional resistance case [Part I (6)], uncoupled from their governing equations of the two reservoirs. A quasi-steady state is reached after a short time within the membrane, and the governing equations become

$$\frac{d^2C}{dx^2} = 0 \tag{15a}$$

$$x = 0; \qquad C = K_{e1}C_{b1} \tag{15b}$$

$$x = l; \qquad C = K_{e2}C_{b2} \tag{15c}$$

The solution of Eq. (15) with the

$$\frac{C - K_{e1}C_{b1}}{(K_{e2}C_{b2}) - (K_{e1}C_{b1})} = \frac{x}{l} \tag{16}$$

Using Fick's law of diffusion, the flux can be expressed as

$$J = -\mathscr{D}_e \frac{\partial C}{\partial x}$$

$$= \frac{\mathscr{D}_e}{l}(K_{e1}C_{b1} - K_{e2}C_{b2}) \tag{17}$$

When the experimental conditions are such that $K_{e1}C_{b1} \gg K_{e2}C_{b2}$, then

$$J = \frac{\mathscr{D}_e}{l} K_{e1} C_{b1} \tag{18}$$

Using the definition of the permeability coefficient, $P = J/C_{b1}$, gives

$$P = \frac{\mathscr{D}_e}{l} K_{e1} \tag{19}$$

By comparing Eq. (19) with Eq. (14), we can consider that

$$K_{e1} = D_1 \tag{20}$$

Danesi et al. (15) assumed that $K_{e1} = k_1/k_{-1} = D_1$, the distribution ratio of the metal species between the liquid membrane and the aqueous extracting solution.

Evaluation of the Parameters

From the model equations and using the experimental data, one should be able to estimate several important parameters of the system such as the effective diffusivity, $\mathscr{D}_e$, the extraction side effective equilibrium constant, K_{e1}, and the stripping side effective equilibrium constant, K_{e2}. Two techniques were used, and the results were compared.

Nonlinear Regression Technique

This technique uses a nonlinear-square optimization function such as the Marquardt algorithm [Kuester and Mize (16), Marquardt (17)]. The method consists of optimizing a least-square objective function of the form

$$F = \sum_{i=1}^{N} (y_i - \bar{y_i})^2 \tag{21}$$

where y_i are the experimental values of the dependent variable and $\bar{y_i}$ are their model estimates. The optimization process of the model is tested by evaluating the value of the least-square objective function F (that is, $F = 0$ for a perfect fit) and by calculating the multiple correlation coefficient R^2 (that is, $R^2 = 1$ for a perfect fit and $R^2 = 0$ for a poor fit).

In order to have good optimization for nonlinear problems, the number of parameters evaluated has to be limited. Our model has been simplified to a three-parameters model as follows:

$$Z = A_1 + A_2 \exp A_3\omega \tag{22}$$

where Z is the dimensionless concentration in either reservoir, ω is the time, and A_1, A_2, and A_3 are the parameters of the model. Once the parameters A_1, A_2, and A_3 are determined, then we can either: a) Estimate the effective diffusivity using the Wilke–Chang equation or the Stokes–Einstein equation [Bird

et al. (18), Wilke (19), Sherwood et al. (20)] as explained in the preceding paper; or b) determine the value of K_{e1} from equilibrium experiments, permeability measurements, or obtain it from the literature. Depending on whether $\mathscr{D}_e$ or K_{e1} is known, the other parameter can be determined from A_3. Also, K_{e2} can be determined from A_1 or A_2 and compared to literature values.

Dynamic Steady-State Experimental Fitting: Using the Slow Time Concept ($\tilde{t}$ − t technique)

This technique uses the experimental results and the steady-state solution to evaluate the unknown parameter in the model equation, β [Part I (6)]. By assuming typical slow times $\tilde{t}$ values, the dependent variable values (the dimensionless concentration) can be calculated, which in turn are compared to the experimental values to extract real time estimates. Since the slow time $\tilde{t}$ is defined in terms of real time t as

$$t = \frac{A}{lv_1} K_{e1} \mathscr{D}_e t \tag{23}$$

Then the slow time values can be plotted against real time values. From the slope of this linear relationship (that is, a straight line passing through the origin as at $t = 0$; $\tilde{t} = 0$) and knowing K_{e1}, the effective diffusivity can be easily obtained [Do et al. (21)]. The advantage of this method is that it gives an estimate of the effective diffusivity using the experimental results.

Using Nondimensional Time (τ − t technique)

The system of equations for fast interfacial reactions with negligible aqueous diffusional resistances case illustrated in Part I can be solved using the nondimensional time instead of the slow time concept. Here, the pseudosteady-state assumption has to be utilized. Since the volume of the membrane matrix is much less than the volume of the reservoirs, then the change of concentration with time must be much less than the change of concentration with position [Cussler (22)]. The solution of this system of equations, which is obtained in a similar way as explained in Part I (6), is written as follows:

$$E = h - (h - \beta g)y \tag{24}$$

$$h = \frac{\beta\left(\gamma + \frac{\alpha'}{\alpha}\right)}{\left(1 + \frac{\alpha'}{\alpha}\beta\right)} + \frac{(1 - \beta\gamma)}{\left(1 + \frac{\alpha'}{\alpha}\beta\right)} e^{-\alpha(1 + \frac{\alpha'}{\alpha}\beta)\tau} \tag{25}$$

$$g = \frac{\left(\gamma + \frac{\alpha'}{\alpha}\right)}{\left(1 + \frac{\alpha'}{\alpha}\beta\right)} - \frac{\frac{\alpha'}{\alpha}(1 - \beta\gamma)}{\left(1 + \frac{\alpha'}{\alpha}\beta\right)} e^{-\alpha(1 + \frac{\alpha'}{\alpha}\beta)\tau} \tag{26}$$

MARCEL DEKKER, INC.
270 Madison Avenue, New York, New York 10016

The advantage of this method is that it gives an estimate of the effective diffusivity using the available experimental results. This method is based on the definition of the nondimensional time τ in Part I (6) as

$$\tau = \frac{\mathcal{D}_e}{l^2} t \tag{27}$$

The following algorithm is used to calculate the effective diffusivity:

1. Obtain K_{e1} either from the literature, from equilibrium experiments, or from permeability measurements by using the relation (Eq. 9) $K_{e1} = Pl/\mathcal{D}_e$. Note that $\mathcal{D}_e$ is assumed or determined from the nonlinear regression technique.
2. Calculate $\alpha = Al K_{e1}/V_1$ for the system.
3. Obtain β from the experimental curve (g vs t) and use the steady-state solution reported in Part I (6).
4. Assume a typical τ and calculate the nondimensional concentration (g) using the model equation.
5. Find the corresponding real time values from the experimental curve.
6. Plot t versus τ (a linear relationship with a slope equal to $\mathcal{D}_e/l^2$ and an intercept of 0 as at $t = 0$; $\tau = 0$).
7. Determine the effective diffusivity, $\mathcal{D}_e$, from the value of the slope.
8. Compare $\mathcal{D}_e$ with the assumed value obtained from the nonlinear regression technique.

Another advantage of this technique ($\tau - t$) is that it gives us an estimate of the Damköhler number which allows us to verify the hypothesis of fast chemical reactions or slow chemical reactions. If the reactions are slow, they must have half-lives much greater than the diffusion time, $l^2/\mathcal{D}_e$.

EXPERIMENTAL

Reagents and Membranes

Two carriers were used as the liquid membrane: Bis(2-ethylhexyl) hydrogen phosphate (denoted by B2EHHP) and tri-*n*-butyl phosphate (denoted by TBP). B2EHHP is manufactured by Aldrich Chemical and TBP is manufactured by Albright & Wilson. The carriers were diluted with Shellsol 2046 manufactured by Shell Chemicals. Shellsol is a high boiling, high flash point hydrocarbon solvent. All aqueous solutions were prepared from reagent-grade chemicals. The extracted solutions were either uranyl nitrate or thorium nitrate dissolved in nitric acid. The stripping solution was sodium carbonate.

The hydrophobic organic phase forming the liquid membrane was immobilized within the pores of Celgard 2500, a microporous polypropylene film made by Celanese Plastics. This membrane is approximately 25 μm thick and

MARCEL DEKKER, INC.
270 Madison Avenue, New York, New York 10016

has a nominal porosity of 45%, with a pore diameter of the order of 0.02 μm. Impregnating the pores of these membranes with the organic solvents was accomplished under vacuum.

Permeability Study

The permeability apparatus consists of two spherical glass vessels, each one having a volume of 500 cm^3 [Elhassadi (23)]. The two vessels are clamped together through two flanges facing each other with a cross-sectional area of 25 cm^2. The membrane is positioned in between the two flanges and protected by two Teflon gaskets. The two vessels are stirred continuously by stainless steel stirrers driven by electric motors. Each compartment was provided with a sampling port, a stirrer port, and a pH-electrode port. The metal ion concentrations of the solution on each side were monitored periodically by taking samples of known volume for analysis. The permeability coefficient was obtained from the concentration versus time data [Elhassadi et al. (23–25)].

Chemical Analysis

Uranium and thorium were determined by EDTA titrations using xylenol orange as an indicator [Kinnunen and Weunerstrand (26), Korbl and Pribil (27)]. Korbl and Pribil (27) suggested that by appropriate pH adjustments certain pairs of metals may be titrated successively in a single sample solution. Kinnunen and Weunerstrand (26) suggested that because of the fewer interferences in acidic solution titrations and the possibility of masking most of them, the EDTA titration reported in their work may be useful in practical analysis. Thus, the binary system was analyzed in one of two ways: a) A sample was divided into two aliquots and each was analyzed for a certain metal, or b) the sample was analyzed first for thorium and then for uranium. It was found that both methods give reasonable results.

RESULTS AND DISCUSSION

The findings of Eqs. (7) and (8) were tested with experimental data, and the results are presented in Tables 1 and 2 and shown in Fig. 1. Table 1 and Fig. 1 show the comparison between the experimental fluxes and theoretical fluxes determined by Eqs. (7) and (8). The equations predict that the slope of the equations should equal $\mathcal{D}_e/l$, the effective diffusivity divided by the membrane thickness. The effective diffusivities were determined from simulating the experimental results using the nonlinear regression technique. The effective equilibrium constants at the extraction interface were obtained from simulating the results of Sato (28, 29) with Eq. (4). The determined membrane thickness values are excellent predictions of the actual membrane thickness of

0.0025 cm. The predicted membrane thicknesses were larger by a factor of 2, which led us to modify the slope to equal $\mathscr{D}_e/2l$. Lee et al.'s (13) determinations of the effective membrane thickness were larger by a factor of 10. This was caused by the use of a free bulk diffusivity instead of a restricted effective diffusivity in the SLM pore structure. As a result of this, their reported diffusion coefficients were larger in magnitude by a constant factor of 10.

The other advantage of Eq. (7) is that the contribution to the flux is determined by both the effective diffusivity and the effective equilibrium constant (K_{e1}) or the effective distribution ratio (D_1) at the extraction interface. Therefore, at higher carrier concentrations, D_1 values are very high according to Eq. (4), and the effective diffusivity values are lowered, which causes the flux to decrease, thus accounting for some of the deviations from the linear behavior of the flux with respect to carrier concentration. This is illustrated very clearly in Case (*c*) in Table 1 for higher carrier concentration values.

Table 2 presents the selective transport of uranium and thorium with respect to time as predicted by Eq. (6) and shown in Fig. 8. The advantage of Eq. (6) over Eq. (8) is that Eq. (6) compares the relative fluxes of the binary system in a dynamic sense rather than a thermodynamic equilibrium sense. This is very important in selective separations because it gives us an idea about the history of the selective separation and when it is best to stop the process. Here, the assumption of equal effective diffusivities was used and was assumed to be equal to the best value obtained in Table 1, i.e., 3.05×10^{-9} cm^2/s. Using the nonlinear regression technique, the data were simulated to determine the effective equilibrium constants values K_{e1}^{U} and K_{e1}^{Th}. The fluxes were calculated using Eq. (3). It was found that the measured fluxes do correlate very closely with the predictions of Eq. (6). The slope in Table 2 equals 2.33, which should be equal to the ratio K_{e1}^{Th}/K_{e1}^{U}. From the permeability measurements we found $P_U = 13.90 \times 10^{-5}$ cm/s and $P_{Th} = 29.67 \times 10^{-5}$ cm/s [that is, P was obtained experimentally from $\ln C/C_0 = -(A\varepsilon/V_1)Pt$]. The ratio P_{Th}/P_U, which is equal to K_{e1}^{Th}/K_{e1}^{U} (Eq. 10), is 2.13. This is in surprisingly good agreement with the value of 2.33. This result shows the important relationship between equilibrium measurements and membrane separations.

The results of parameter evaluation for the single system using a) the nonlinear regression technique and b) the dynamic steady-state experimental fitting technique are presented in Table 3 and shown in Figs. 2–6. The data simulated are those of Matsuoka et al. (30), Akiba and Kanno (31), and this work. Figures 2–6 show that the three-parameter nonlinear regression model, Eq. (22), simulates the experimental results very closely. Table 3 compares the effective diffusivity values obtained using the two-parameter evaluation techniques. It can be seen that the two-parameter evaluation techniques give good and equal estimates of $\mathscr{D}_e$. The bulk diffusion coefficient in free solution, D_0, was estimates from the Stokes–Einstein equation to be equal to 7×10^{-7}

TABLE 1
Comparison between Experimental Fluxes and Theoretical Fluxes for Uranium and Thorium Single Systems

Carrier (10^{-3} mol · cm^3)	K_{el}	$\mathcal{D}_e$ (10^{-9} cm^2/s)	P (10^{-5} cm/s)	$J_{exp} = C_{b10}P$ (10^{-10} mol/cm^2·s)	$J_{model} = (\mathcal{D}_e/l)C_{b10}K_{el}$ (10^{-10} mol/cm^2·s)	Remarks[a]
			(a) Uranium			
0	0	—	1.70	1.79	0	Extraction side solution = 1.00 M HNO_3
0.15	5.96	11.19	3.29	3.46	2.80	Strip side solution = 1.0 M Na_2CO_3
1.20	381.68	0.45	10.28	10.79	7.24	C_{b10} = 0.01 M; $\mathcal{D}_e = 3.05 \times 10^{-9}$ cm^2/s
1.50	596.30	0.30	12.27	12.88	7.44	
2.10	1,168.8	0.25	13.48	14.15	12.27	
3.00	2,385.4	0.21	3.0	3.15	21.04	
			(b) Uranium			
0	0	—	1.65	1.88	0	Extraction side solution = 1.0 M HNO_3
0.15	5.96	21.5	2.98	3.40	5.84	Strip side solution = 1.00 M Na_2CO_3
0.30	23.86	5.23	3.60	4.10	5.69	C_{b10} = 0.013 M; $\mathcal{D}_e = 5.38 \times 10^{-9}$ cm^2/s
0.60	95.42	1.60	5.37	6.12	6.96	
0.90	214.70	1.34	7.38	8.41	13.12	
1.50	596.30	0.44	9.77	11.14	11.96	
3.00	2,385.4	0.096	2.45	2.79	10.44	
			(c) Thorium			
0	0	—	0	0	—	Extraction side solution = 2 M HNO_3
0.15	463	—	0	0	—	Strip side solution = 2 M Na_2CO_3
0.30	1,855	2.25	0.73	0.59	13.52	C_{b10} = 0.0081 M; assume $\mathcal{D}_e = 3.05 \times 10^{-9}$ cm^2/s
0.60	7,420	0.090	2.06	1.67	2.16	
0.90	16,694	0.087	4.92	3.99	4.72	
1.20	29,678	0.031	6.46	5.23	6.02	
1.50	46,366	0.031	7.74	6.27	4.63	
2.10	90,881	0.025	5.62	4.55	7.33	
3.00	185,477	0.008	2.00	1.62	4.77	

	Experimental	Model
R^2	0.9830	0.9737
a	2.5×10^{-10}	1.72×10^{-10}
b	6.18×10^{-7}	4.63×10^{-7}
l	0.0025	0.0033

	Experimental	Model
R^2	0.9676	0.85
a	2.5×10^{-10}	4.85×10^{-10}
b	6.20×10^{-7}	5.61×10^{-7}
l	0.0043	0.0048

	Experimental	Model
R^2	0.9889	0.83
a	5.18×10^{-11}	4.0×10^{-11}
b	4.6×10^{-7}	3.36×10^{-7}
l	0.0033	0.0045

[a] a = intercept; b = slope = $\mathcal{D}_e/2l$; l = determined membrane thickness; $\overline{\mathcal{D}}_e$ = average diffusivity of all values; $\mathcal{D}_e$ was obtained from the non-linear regression technique; P was obtained experimentally from $\ln \frac{C}{C_0} = -\left(\frac{A_\epsilon}{V}\right) Pt$.

MARCEL DEKKER, INC.
270 Madison Avenue, New York, New York 10016

TABLE 2
Selective Transport of Uranium and Thorium with Respect to Time as Predicted by Eq. (7) and Shown in Fig. 8

h		g		$h-g$		J (10^{-10} mol/cm^2·s)		
U	Th	U	Th	U	Th	U	Th	Remarks
1.0	1.0	0.0	0.0	1.0	1.0	3.90	6.65	$ß_U = 0.004$
0.93	0.86	0.07	0.14	0.929	0.853	3.63	5.59	$ß_{Th} = 0.048$
0.86	0.73	0.14	0.27	0.859	0.717	3.35	4.70	$\mathscr{D}_e^U = \mathscr{D}_e^{Th} = 3.05 \times 10^{-9}$ cm^2/s
0.80	0.62	0.20	0.38	0.799	0.602	3.12	3.94	$K_{e1}^U = 56.95$, $\frac{K_{e1}^{Th}}{K_{e1}^U} = 2.31$
0.75	0.53	0.25	0.47	0.749	0.507	2.92	3.32	$K_{e1}^{Th} = 131.60$,
0.69	0.44	0.31	0.56	0.689	0.413	2.69	2.71	$C_{b10}^U = 5.62 \times 10-6$ mol/cm^3
0.64	0.37	0.36	0.63	0.639	0.340	2.50	2.23	$C_{b10}^{Th} = 4.08 \times 10^{-6}$ mol/cm^3
0.59	0.32	0.41	0.68	0.588	0.287	2.30	1.88	
0.55	0.26	0.45	0.74	0.548	0.224	2.14	1.47	$J = \frac{\mathscr{D}_e}{l} C_{b10} K_{e1} (h-g)$
0.51	0.22	0.49	0.78	0.508	0.183	1.98	1.20	
0.46	0.19	0.54	0.81	0.458	0.151	1.79	0.99	$\frac{J_M}{J_N} = \frac{C_{b10}^M K_{e1}^M}{C_{b10}^N K_{e1}^N} \frac{(h-g)_M}{(h-g)_N}$
0.41	0.15	0.60	0.85	0.408	0.109	1.59	0.71	
0.35	0.11	0.65	0.89	0.347	0.067	1.35	0.44	$R^2 = 0.9998$
0.29	0.10	0.71	0.90	0.287	0.057	1.12	0.37	$a = -0.0028$
0.25	0.10	0.75	0.90	0.247	0.057	0.96	0.37	$b = 1.69 = \frac{C_{b10}^{Th} K_{el}^{Th}}{C_{b10}^U K_{e1}^U}$
0.23	0.09	0.77	0.91	0.227	0.046	0.89	0.30	$\frac{K_{e1}^{Th}}{K_{e1}^U} = 2.33$

cm^2/s. The ratio $\overline{\mathscr{D}}_e/D_0$ obtained in Table 2 has the same order of magnitude and is characteristic of systems of preferentially adsorbed solutes obtained by Satterfield et al. (32). The discrepancy between the ratio $\overline{\mathscr{D}}_e/D_0$ and the ratio $\varepsilon' K_r K_p/\tau'$ [used in the definition of the effective diffusivity in Part I (6)] is characteristic of adsorbed solutes and is accounted for by the two mechanisms of diffusion in a porous medium. That is, diffusion in the volume of the fluid filling the pores and surface diffusion in the adsorbed layer on the pore walls [Satterfield et al. (32), Reikart (33), Komiyama and Smith (34), Aris (35)]. A discussion of these effects is not included in this paper. The twelfth column in Table 3 shows the Damköhler number ($l^2/\mathscr{D}_e t_s$), where t_s is a characteristic reaction time. For most cases the Damköhler numbers within the membrane are very large ($l^2/\mathscr{D}_e t_s \gg 1$), implying that diffusion across the membrane is the

MARCEL DEKKER, INC.
270 Madison Avenue, New York, New York 10016

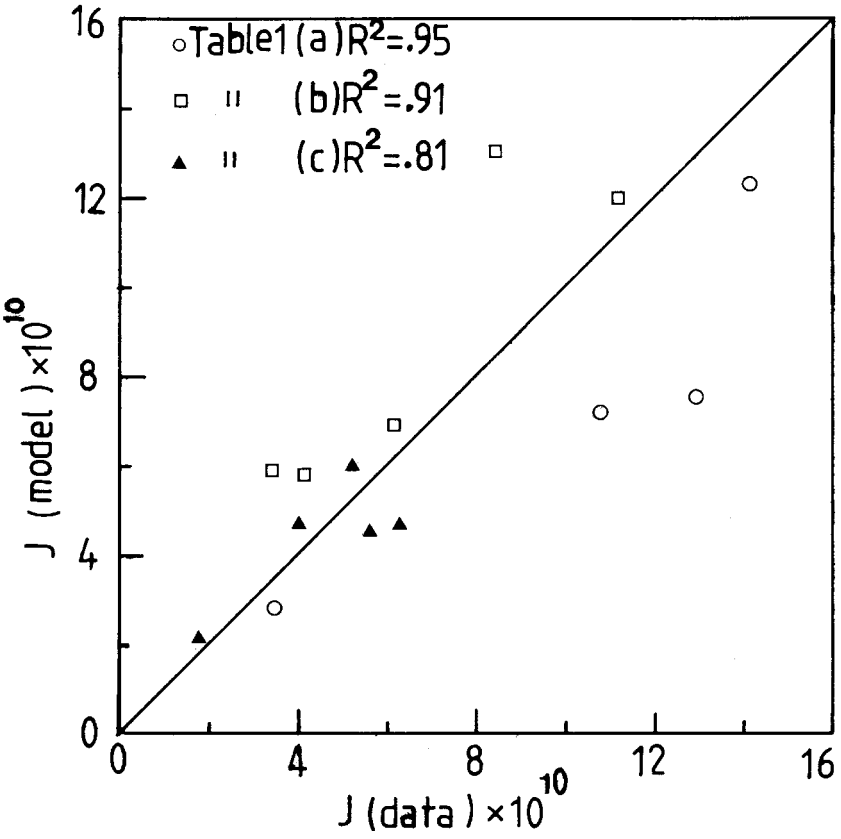

FIG. 1 Comparison between experimental and theoretical fluxes for uranium and thorium single systems.

only resistance to mass transfer. No direct measure of this characteristic time is available. The reported values of t_s in the literature are of the order of 10^{-6} second [Reusch and Cussler (36)]. The last column in Table 3 reports some values for the tortuosity using the two relations $\tau = (\mathscr{D}_e/D_0)^{-1}\varepsilon' K_r K_p$ and $\tau = \sqrt{\varepsilon \mathscr{D}_e/D_0}$ [reported by Duffey et al. (37)].

The results of the parameter evaluation for the binary system using a) the nonlinear regression technique and b) the dynamic-steady-state experimental fitting technique are presented in Table 4 and shown in Figs. 7–10. Figures 7–10 show the good fit of the three-parameter nonlinear regression model in simulating the experimental data. The aim of Table 4 is to check the assumption that all species within the membrane have equal effective diffusivities. The effective equilibrium constants were obtained experimentally from permeability measurements using the relation $K_e = Pl/\mathscr{D}_e$ (Eq. 9), where $\mathscr{D}_e$ was assumed to equal the best value which gave the exact membrane thickness (i.e., $\mathscr{D}_e = 3.05 \times 10^{-9}$ cm^2/s). It can also be seen that the two-parameter evaluation techniques give good and equal estimates of effective diffusivity. The

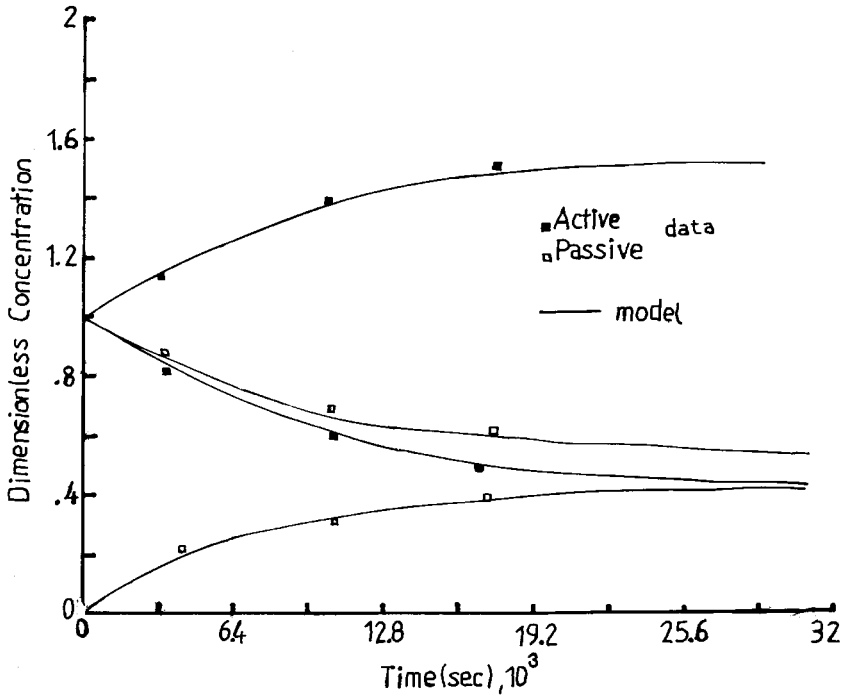

FIG. 2 Simulation of the dimensionless concentration of the extraction side and the strip side versus time (seconds) of Matsuoka et al. (30).

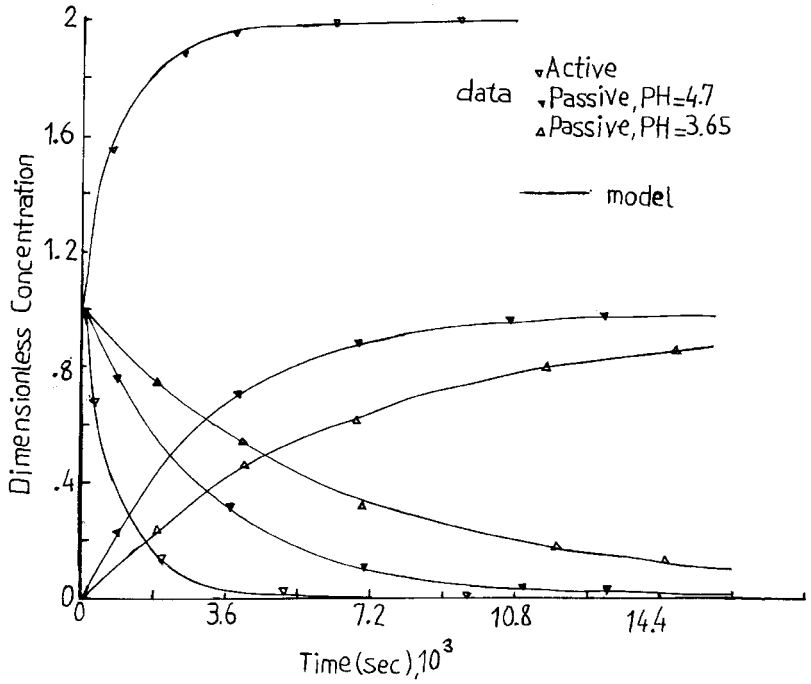

FIG. 3 Simulation of the dimensionless concentration of the extraction side and the strip side versus time (seconds) of Akiba and Kanno (31) results (active and two passive cases of uranium system).

MARCEL DEKKER, INC.
270 Madison Avenue, New York, New York 10016

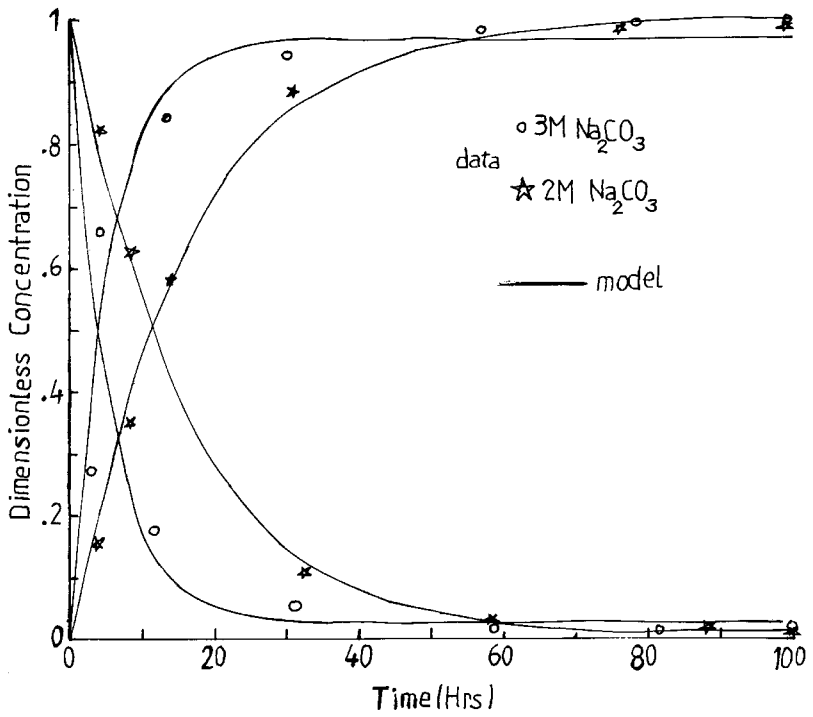

FIG. 4 Simulation of the dimensionless concentration of the extraction side and the strip side versus time (hours) of this work (two passive cases of uranium system). Extraction solution: 5 g/L $UO_2(NO_3)_2$, 6 M HNO_3. Liquid membrane: 30 V/V% B2EHHP in Shellsol. Strip solution: 3 M Na_2CO_3, 2 M Na_2CO_3.

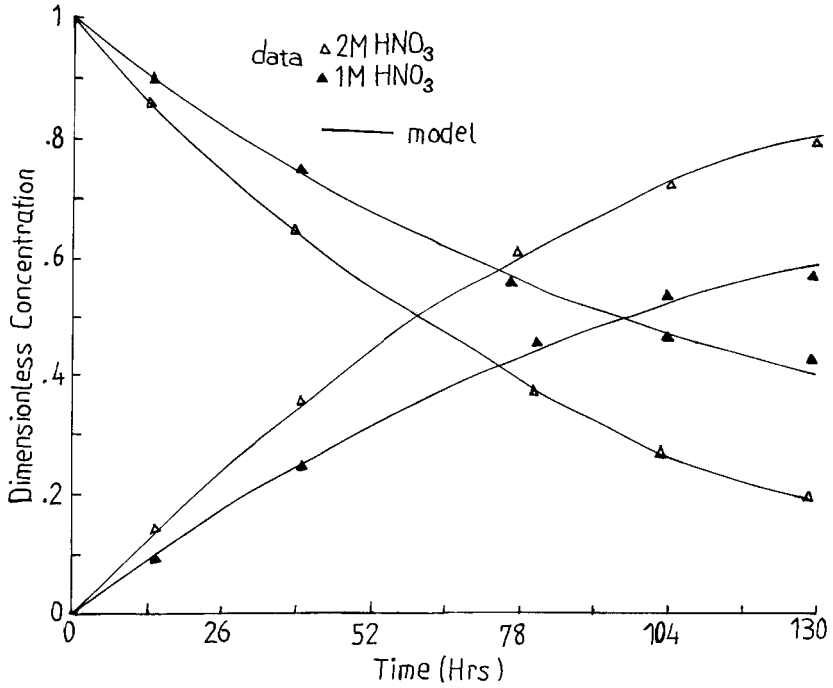

FIG. 5 Simulation of the dimensionless concentration of the extraction side and the strip side versus times (hours) of this work (two passive cases of thorium system). Extraction solution: 1.48 g/L $Th(NO_3)_4$, 2 M HNO_3; 02.56 g/L $Th(NO_3)_4$, 1 M HNO_3. Liquid membrane: 30 V/V% B2EHHP in Shellsol. Strip solution: 2 M Na_2CO_3.

MARCEL DEKKER, INC.
270 Madison Avenue, New York, New York 10016

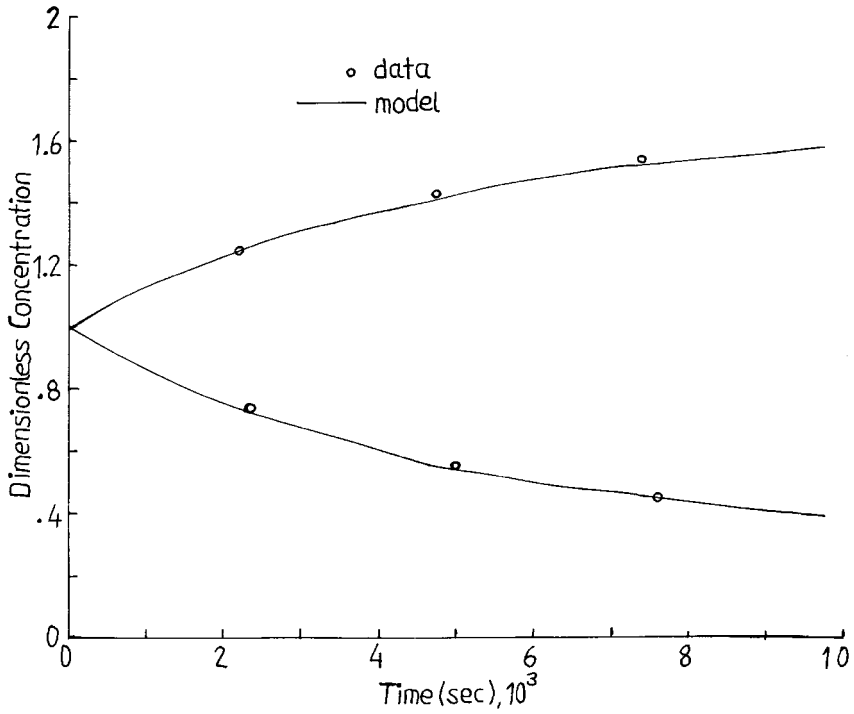

FIG. 6 Simulation of the dimensionless concentration of the extraction side and the strip side versus times (hours) of this work (active case of uranium). Extraction solution: 10 g/L $UO_2(NO_3)$, 1 M HNO_3. Liquid membrane: 100% TBP. Strip solution: 1 M Na_2CO_3.

ratio of the two effective diffusivities in the binary system, $\overline{\mathcal{D}}_e{}^{Th}/\overline{\mathcal{D}}_e{}^{U}$, was found to agree with the assumption that all the species within the SLM have equal effective diffusivities. The effective diffusivity values of thorium varied by two to three times the effective diffusivity of uranium. Lee et al. (13) reported that diffusion coefficient values are assumed to be equal if they remain constant within about $\pm 20\%$. This is in good agreement with the obtained ratio of $\overline{\mathcal{D}}_e{}^{Th}/\overline{\mathcal{D}}_e{}^{U}$ in Table 4. The Damköhler numbers reported in Table 4 for the binary system are very large and consolidate the validity of the assumption that diffusion within the membrane in these cases is the controlling mechanism. If one also looks at the ratio $\overline{\mathcal{D}}_e/D_0$ in Table 4 for the case of the binary system, assuming D_0 is equal to the calculated value of 7×10^{-7} cm^2/s, one would conclude that this ratio has the same order of magnitude and is characteristic of systems of preferentially adsorbed solutes obtained by Satterfield et al. (32). Tables 5(a), 5(b), and 5(c) show a sample calculation on the results presented in Fig. 10, comparing the two methods of parameter evaluation.

After presenting these results, we conclude that the following assumptions have been verified: 1) The assumption that the membrane is the only resistance

TABLE 3
Parameter Evaluation Using the Nonlinear Regression Technique (I) and the

System	Solute	Solvent	K_{e1}	α	β	K_{e2}
Matsuoka et al. (30) Passive Fig. 2	Uranium	TBP TAC membrane	10[a]	0.0025	0.926	9.26
Matsuoka et al. (30) Active Fig. 2	Uranium	TBP TAC membrane	10[a]	0.0025	0.194	1.94
Akiba et al. (31) Passive; pH 3.65, Fig. 3	Uranium	LIX63 in kerosene	10[a]	0.039	0.9435	9.435
Akiba et al. (31) Passive; pH 4.7, Fig. 3	Uranium	LIX63 in kerosone	10[a]	0.039	0.9052	9.052
Akiba et al. (31) Active Fig. 3	Uranium	LIX63 in kerosene	10[a]	0.0975	0.0035	0.035
Ours; passive Fig. 4	Uranium	B2EHHP Shellsol Celgard 2500	729.10[†]	0.091	0.0303	22.09
Ours; passive Fig. 4	Uranium	B2EHHP Shellsol Celgard 2500	729.10[†]	0.091	0.0212	15.46
Ours; passive Fig. 5	Thorium	B2EHHP Shellsol Celgard 2500	126.80[†]	0.016	0.1899	24.08
Ours; passive Fig. 5	Thorium	B2EHHP Shellsol Celgard 2500	70.49[†]	0.016	0.1468	10.35
Ours; active Fig. 6	Uranium	TBP	10[a]	0.0013	0.2026	2.03

[a] Obtained from Matsuoka et al. (30).

[b] $\tau = \sqrt{\mathcal{D}_0/\mathcal{D}_e}$ (Duffey et al., 39) obtained experimentally from $k_{e1} = Pl/\mathcal{D}_e$, where $\mathcal{D}_e = 3.05 \times 10^{-9}$ cm^2/s.

[c] $\overline{\mathcal{D}}_e/\mathcal{D}_0 = \varepsilon^1 k_r k_p/\tau$.

to mass transfer because of the large Damköhler numbers obtained. 2) The slow time concept assumption that α is a very small number (i.e., $\alpha \ll 1$). From the reported values in Table 3, one can see that $\alpha \ll 1$. 3) The assumption that the effective diffusivities are equal is valid because their variations are constant within ±20%. 4) The assumption that the permeability measurements can provide an effective guide for estimating the effective equilibrium constant K_{e1} and

MARCEL DEKKER, INC.
270 Madison Avenue, New York, New York 10016

Steady-State Dynamic Experimental Fitting (II). Single Systems

$\mathscr{D}_e^I$	$\mathscr{D}_e^{II}$	$\mathscr{D}_0$	$\mathscr{D}_e/\mathscr{D}_0$	$\frac{l^2}{\mathscr{D}_e^I t_s}(10^6)$	τ	Remarks
2.37×10^{-8}	1.45×10^{-8}	7×10^{-7}	0.027	68.97	4.08[b]	$A = 0.5$ cm^2 $l = 1 \times 10^{-3}$ cm $V_1 = 2$ mL
2.64×10^{-8}	5.06×10^{-8}	7×10^{-7}	0.055	19.76	2.86[b]	$A = 0.5$ cm^2 $l = 1 \times 10^{-3}$ cm $V_1 = 2$ mL
9.26×10^{-8}	1.38×10^{-7}	7×10^{-7}	0.165	66.67	4.45[c]	$A = 26$ cm^2 $l = 0.015$ cm $V_1 = 100$ mL
6.54×10^{-8}	1.66×10^{-7}	7×10^{-7}	0.165	1.64×10^3	4.45[c]	$A = 26$ cm^2 $l = 0.015$ cm $V_1 = 100$ mL
2.44×10^{-6}	2.03×10^{-6}	7×10^{-7}	—	111.11	n/a	$A = 26$ cm^2 $l = 0.015$ cm $V_1 = 40$ mL
3.76×10^{-9}	2.11×10^{-9}	7×10^{-7}	0.004	2.94×10^3	n/a	$A = 25$ cm^2 $l = 0.0025$ cm $V_1 = 500$ mL
1.21×10^{-9}	1.49×10^{-9}	7×10^{-7}	0.002	4.17×10^3	n/a	$A = 25$ cm^2 $l = 0.0025$ cm $V_1 = 500$ mL
8.67×10^{-10}	1.52×10^{-9}	7×10^{-7}	0.002	4.17×10^3	n/a	$A = 25$ cm^2 $l = 0.0025$ cm $V_1 = 500$ mL
1.61×10^{-9}	1.85×10^{-9}	7×10^{-7}	0.0025	3.38×10^3	n/a	$A = 25$ cm^2 $l = 0.0025$ cm $V_1 = 500$ mL
9.21×10^{-7}	1.34×10^{-6}	7×10^{-7}	—	4.67	n/a	$A = 25$ cm^2 $l = 0.0025$ cm $V_1 = 500$ mL

the effective diffusivity $\mathscr{D}_e$, which could be easily checked with reported literature values. The estimated effective diffusivity value of 3.05×10^{-9} cm^2/s, which gave a good estimate of effective membrane thickness, was found to give good estimates of K_{e1} which compare excellently with the literature values.

Table 4 also shows that the selectivity of the SLM is enhanced depending on the way one tailors these membranes. We found B2EHHP to be very se-

MARCEL DEKKER, INC.
270 Madison Avenue, New York, New York 10016

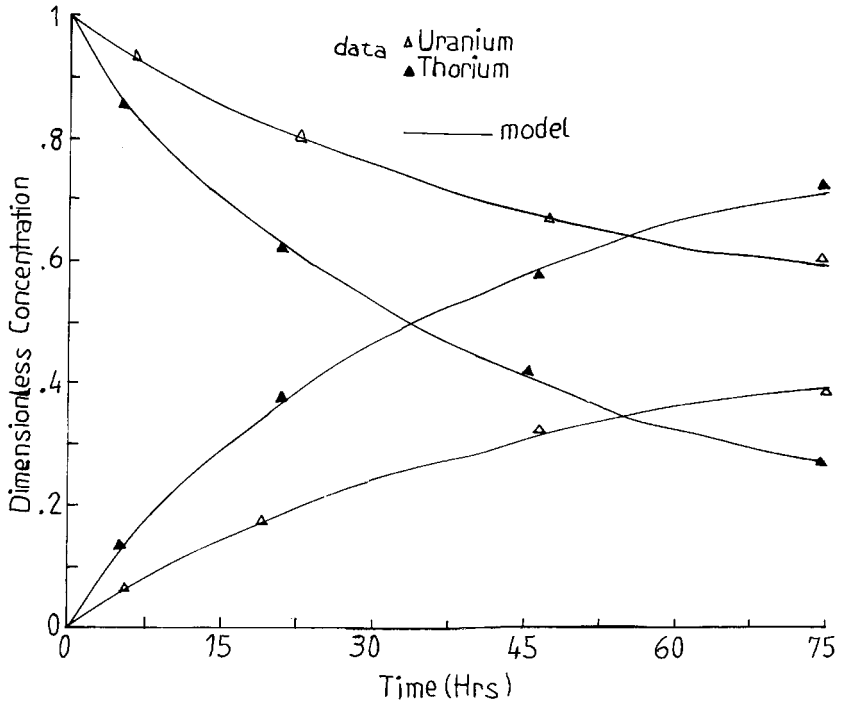

FIG. 7 Simulation of the dimensionless concentration of the extraction side and the strip side versus time (hours) of this work (binary system of uranium and thorium). Extraction solution: 5 g/L $UO_2(NO_3)_2$, 5 g/L $Th(NO_3)_4$, M HNO_3. Liquid membrane: 30 V/V% B2EHHP in Shellsol. Strip solution: 4 M Na_2CO_3.

lective to thorium, and TBP to be very selective to uranium. For the single metal system and using a mixture of the two carriers, the flux at first rises steeply with the mixed carrier concentration, then passes through a maximum which appears at a mole ratio of [(selective carrier concentration)/(less selective carrier concentration)] equal to 1, and then decreases gradually [Sato et al. (38, 39)]. For the binary metal system, the selectivity behavior is quite complex. An understanding of the synergic effect of two carriers and the complex interactions of multicomponent metal systems is required. We believe that further work is necessary to better demonstrate the concepts of these selectivities and tailoring.

In the cases of active transport, the effective diffusivities were found to have a large order of magnitude of 10^{-6} to 10^{-7} cm^2/s. The causes behind this increase are not well understood as there is no convincing explanation of these systems in terms of a well-defined chemical mechanism [Cussler (22)]. However, the new model was capable of characterizing and simulating the behavior of this active transport to some extent.

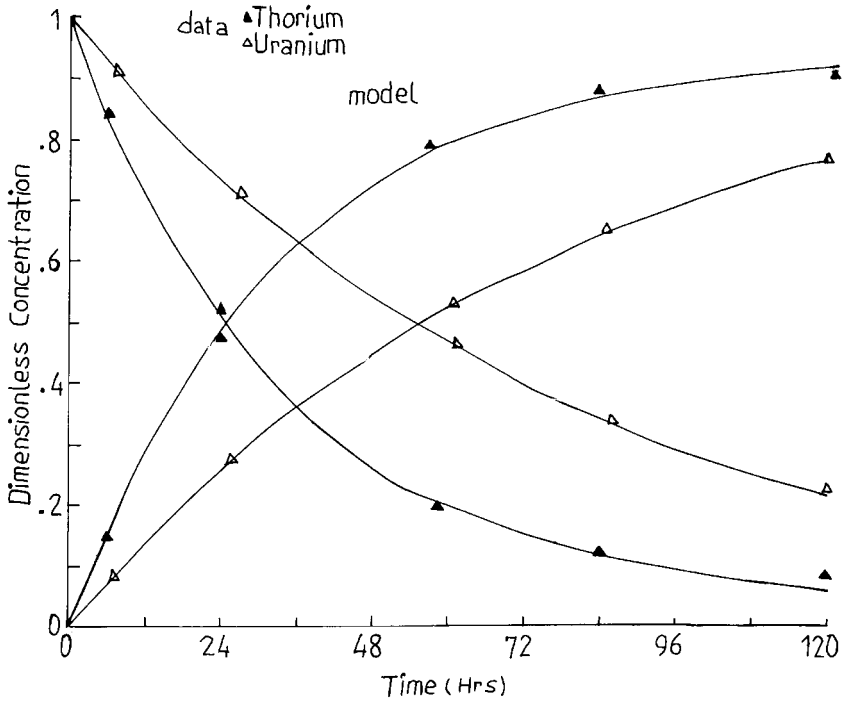

FIG. 8 Simulation of the dimensionless concentration of the extraction side and the strip side versus time (hour) of this work (binary system of uranium and thorium). Extraction solution: 2.83 g/L $UO_2(NO_3)_2$, 2.46 g/L $Th(NO_3)_4$. Liquid membrane: 80 V/V% B2EHHP, 10 V/V% TBP in Shellsol. Strip solution: 2 M Na_2CO_3.

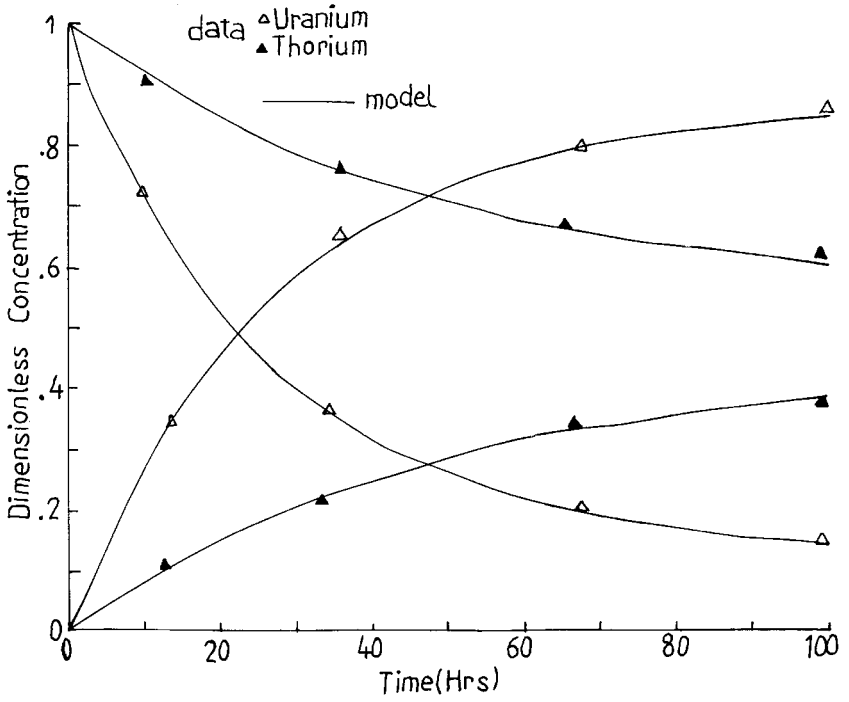

FIG. 9 Simulation of the dimensionless concentration of the extraction side and the strip side versus time (hours) of this work (binary system of uranium and thorium). Extraction solution: 3.72 g/L $UO_2(NO_3)_2$, 2.76 g/L $Th(NO_3)_4$, 2 M HNO_3. Liquid membrane: 50 V/V% TBP in Shellsol. Strip solution: 2 M Na_2CO_3.

MARCEL DEKKER, INC.
270 Madison Avenue, New York, New York 10016

TABLE 4
Parameter Evaluation Using the Nonlinear Regression Technique (I) and

System	Solute	Solvent	K_{e1}[a]		α		β		K_{e2}	
			U	Th	U	Th	U	Th	U	Th
Ours; passive Fig. 7	Uranium + thorium	B2EHHP	65.57	165.33	0.0082	0.021	0.19	0.98	12.46	162.02
Ours; passive Fig. 8	Uranium + thorium	B2EHHP + TBP	114.26	243.20	0.014	0.030	0.004	0.048	0.46	11.67
Ours; passive Fig. 9	Uranium thorium	TBP	157.62	47.79	0.02	0.006	0.15	1.28	23.64	61.17
Ours; passive Fig. 10	Uranium + thorium	TBP + B2EHHP	247.79	82.54	0.03	0.01	0.24	1.01	59.47	83.37

[a] k_{e1} was obtained experimentally from permeability measurements by $k_{e1} = Pl/\mathcal{D}_e$, where $\mathcal{D}_e = 3.05 \times 10^{-9}$ cm^2/s.

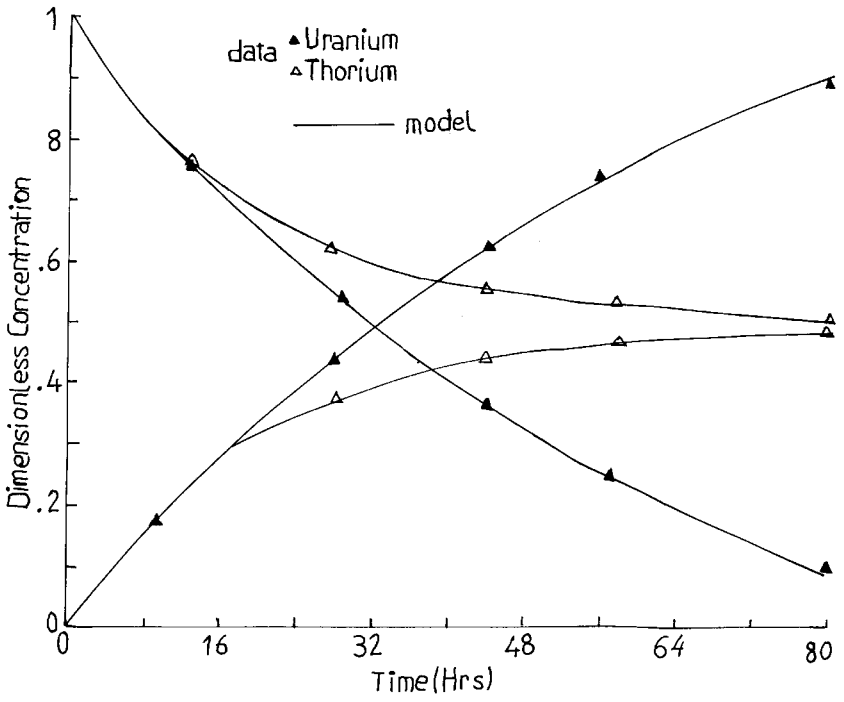

FIG. 10 Simulation of the dimensionless concentration of the extraction side and the strip side versus time (hours) of this work (binary system of uranium and thorium). Extraction solution: 2 g/L $UO_2(NO_3)_2$, 2 g/L $Th(NO_3)_4$, 8 M HNO_3. Liquid membrane: 38.1 V/V% TBP, 4.8 V/V% B2EHHP in Shellsol. Strip solution: 1 M Na_2CO_3.

MARCEL DEKKER, INC.
270 Madison Avenue, New York, New York 10016

the Steady-State Dynamic Experimental Fitting (II). Binary System

$\mathcal{D}_e^I$		$\mathcal{D}_e^{II}$		Selective	$\frac{\bar{\mathcal{D}}_e^{Th}}{\bar{\mathcal{D}}_e^{U}}$	$l^2/\mathfrak{D}_e t_s$ (10^6)		
U	Th	U	Th	T_0		U	Th	Remarks
4.58×10^{-9}	7.90×10^{-10}	9.13×10^{-10}	1.75×10^{-9}	Thorium	3.2	7.7×10^{2}	3.3×10^{3}	$A = 25\ cm^2$ $l = 0.0025$ $V_1 = 500\ mL$
1.52×10^{-9}	2.96×10^{-9}	1.65×10^{-9}	2.53×10^{-9}	Thorium	2.6	2.1×10^{3}	2.5×10^{3}	$A = 25\ cm^2$ $l = 0.0025$ $V_1 = 500\ mL$
2.88×10^{-9}	3.06×10^{-9}	2.75×10^{-9}	3.93×10^{-9}	Uranium	1.8	2.0×10^{3}	1.6×10^{3}	$A = 25\ cm^2$ $l = 0.0025$ $V_1 = 500\ mL$
6.65×10^{-10}	1.71×10^{-9}	4.23×10^{-9}	9.01×10^{-9}	Uranium	2.6	3.7×10^{3}	7.1×10^{2}	$A = 25\ cm^2$ $l = 0.0025$ $V_1 = 500\ mL$

TABLE 5(a)
Calculation Sample on the Results Presented in Fig. 10, Comparing the Two Methods of Parameter Evaluation: Nonlinear Regression Technique[a]

A_1		A_2		A_3		$\mathcal{D}_e^I$	
U	Th	U	Th	U	Th	U	Th
0.81	0.499	−0.81	−0.497	4.09×10^{-6}	1.4×10^{-5}	6.65×10^{-10}	4.23×10^{-9}

$$^aA_1 = \frac{\frac{V_1}{V_2} + \frac{C_{b20}}{C_{b10}}}{1 + \frac{V_1}{V_2} \cdot \frac{K_{e2}}{K_{e1}}}$$

$$A_2 = -\frac{\frac{V_1}{V_2}\left(1 - \frac{K_{d2}C_{b20}}{K_{d1}C_{b10}}\right)}{1 + \frac{V_1K_{e2}}{V_2K_{e1}}}$$

$$A_3 = \left(1 + \frac{V_1K_{e2}}{V_2K_{e1}}\right)\frac{A}{V_1 l} K_{e1}\mathcal{D}_e$$

$V_1 = V_2 = 500$ mL
$C_{b20} = 0$
$A = 25\ cm^2$
$l = 0.0025$ cm
$K_{e1}^U = 247.79; \quad K_{e1}^{Th} = 82.54$

MARCEL DEKKER, INC.
270 Madison Avenue, New York, New York 10016

TABLE 5(b)
Calculation Sample on the Results Presented in Fig. 10, Comparing the Two Methods of Parameter Evaluation: Steady-State Dynamic Experimental Fitting

τ		g		$t \times 10^{-3}$ (s)
0	0	0	0	0
2.7	17.4	0.08	0.08	14.4
8.2	57.8	0.22	0.22	43.2
3.8	105.0	0.34	0.33	72
19.5	143.0	0.44	0.38	100.8
26.6	172.3	0.54	0.41	129.6
39.7	232.9	0.67	0.45	172.8
66.9	332.5	1.81	0.49	230.4

TABLE 5(c)
Calculation Sample on the Results Presented in Fig. 10, Comparing the Two Methods of Parameter Evaluation[a]

R^2		Intercept		Slope		$\mathcal{D}_e^{II}$	
U	Th	U	Th	U	Th	U	Th
0.9793	0.9989	−3.97	−4.20	0.0027	0.0014	1.71×10^{-9}	9.01×10^{-9}

[a] $\alpha^{U} = \dfrac{Alk_{e1}^{U}}{V_1} = .031$; $\alpha^{Th} = \dfrac{AlK_{e1}^{Th}}{V_1} = .01$

$g_\infty = 0.90$; $g_\infty = .50$

$$g_\infty = \frac{V_1/V_2}{1 + \dfrac{V_1 K_{e2}}{V_2 K_{e1}}}$$

CONCLUSIONS

We have simulated the concentration-time experimental curves of 10 single metal ion transport systems across SLH (five of which are from the literature) and four selective binary systems. An effective diffusivity of magnitude 3.05×10^{-9} cm^2/s was found to give excellent values of effective membrane thickness, much better than the estimated diffusion coefficient reported by Lee et al. (13). The ratio of effective diffusivity to bulk free diffusivity was found to characterize systems of strong adsorption within the fine pores of the membrane.

MARCEL DEKKER, INC.
270 Madison Avenue, New York, New York 10016

The two methods used for evaluating the parameters of the system were found to give good estimates of the parameters and to agree quite reasonably with each other. The nonlinear regression technique simulated many dynamic experimental results quite closely.

REFERENCES

1. A. G. Kopp, R. J. Marr, and F. E. Moser, "A New Concept for Mass Transfer in Liquid Surfactant Membranes without Carriers and with Carriers That Pump," *Inst. Chem. Eng. Symp. Ser., 54*, 279–290 (1978).
2. R. Marr and A. Kopp, "Liquid Membrane Technology, A Survey of Phenomena, Mechanisms and Models," *Int. Chem. Eng., 22*, 44–60 (1982).
3. C. G. Chan and C. J. Lee, "Mechanistic Models of Mass Transfer across a Liquid Membrane: Review," *J. Membr. Sci., 20*, 1 (1984).
4. A. M. Darbi, "Transport of Iron across SLM," M.S. Thesis, University of Garyounis, Benghazi, Libya, 1994.
5. N. M. Hassan, "Transport of Manganese across SLM," M.S. Thesis, University of Garyounis, Benghazi, Libya, 1995.
6. A. A. Elhassadi and D. D. Do, "Modeling of the Mass Transfer Rates of Metal Ions across Supported Liquid Membranes. Part I. Theory," *Sep. Sci. Technol., 34*(2), 305–329 (1999).
7. Z. V. P. Murthy and S. K. Gupta, "Simple Graphical Method to Estimate Membrane Transport Parameters and Mass Transfer Coefficients in a Membrane Cell," *Ibid., 31*(1), 77–94 (1996).
8. G. Zuo, S. Orecchio, and M. Muhammed, "Facilitated Transport of Gold through a Membrane via Complexation to Thiourea-Based Reagents," *Ibid., 31*(1), 1597–1613 (1996).
9. R. Wodzki and G. Sionkowski, "Recovery and Concentration of Metal Ions. III. Concentration and Temperature Effects in Multimembrane Hybrid Systems," *Ibid., 31*(1), 1541–1553 (1996).
10. K. Kondo and M. Matsumoto, "Solvent Extraction of Europium with Diisostearylphosphoric Acid and Its Application to an Emulsion Liquid Membrane Technique," *Ibid., 31*(1), 557–567 (1996).
11. U. S. Vural, "The Transport Properties of Metal Picrates by Two New Calixarene Types," *Ibid., 31*(1), 787–798 (1996).
12. M. Ishiguro, T. Matsuura, and C. Detellier, "A Study on the Solute Separation and the Pore Size Distribution of a Montmorillonite Membrane," *Ibid., 31*(1), 545–556 (1996).
13. K. H. Lee, D. F. Evans, and E. L. Cussler, "Selective Copper Recovery with Two Types of Liquid Membranes," *AIChE J., 24*, 860–868 (1978).
14. P. R. Danesi, E. P. Horwitz, G. F. Vandergrift, and P. Chiarizia, "Mass Transfer Rate through Liquid Membrane: Interfacial Chemical Reactions and Diffusion as Simultaneous Permeability Controlling Factors," *Sep. Sci. Technol., 16*, 201–211 (1981).
15. P. R. Danesi, R. Chiarizia, and A. Castagnola, "Transfer Rate and Separation of Cd(II) and Zn(II) Chloride Species by a Trilauryl Ammonium Chloride–Triethyl Benzene SLM," *J. Membr. Sci., 14*, 161–175 (1983).
16. J. L. Kuester and J. H. Mize, *Optimization Techniques with Fortran*, McGraw-Hill, New York, NY, 1973.
17. D. M. Marquardt, "An Algorithm for Least-Squares Estimation of Nonlinear Parameters," *J. Soc. Ind. Appl. Math., 11*, 431 (1963).
18. R. B. Bird, W. E. Stewart, and E. N. Lightfoot, *Transport Phenomena*, Wiley, New York, NY, 1960.

19. C. R. Wilke, *Chem. Eng. Prog.*, *45*, 218 (1949).
20. T. K. Sherwood, R. L. Pigford, and C. R. Wilke, *Mass Transfer*, McGraw-Hill, New York, NY, 1975.
21. D. D. Do, G. V. Bhasker, A. A. Elhassadi, and P. R. Johnston, *Calculation of Effective Diffusivity and Tortuosity for a Phenol–Water–Activated Carbon System Using a Batch Adsorber*, Unpublished Results, 1983.
22. E. L. Cussler, *Multicomponent Diffusion* (Chemical Engineering Monographs, Vol. 3), Elsevier, New York, NY, 1976.
23. A. A. Elhassadi, "Review of the Applications and Models of Membranes Transport Phenomena," in *Environmental Conference Proceedings*, Benghazi, Libya, 1997.
24. A. A. Elhassadi and A. M. Darbi, "Transport of Metals across Supported Liquid Membranes. I. Solubility Mechanism for Iron and Manganese," *Sep. Sci. Technol.*, Submitted.
25. A. A. Elhassadi and N. M. Hassan, "Transport of Metals across Supported Liquid Membranes, II. *Ibid.*, Submitted.
26. J. Kinnunen and B. Weunerstrand, "Some Further Applications of Xylenol Orange as an Indicator in the EDTA Titrations," *Chemist-Analyst*, *46*, 92 (1957).
27. J. Korbl and R. Pribil, "Xylenol Orange: New Indicator for the EDTA Titration," *Ibid.*, *45*, 102 (1966).
28. T. Sato, "The Extraction of Uranium(VI) from Nitric Acid Solutions by Di-(2-ethylhexyl) Phosphoric Acid," *J. Inorg. Nucl. Chem.*, *25*, 109–115 (1963).
29. T. Sato, "The Synergic Effect of TBP in the Extraction of U(VI) from Sulphuric Acid Solutions by Di-(2-ethylhexyl) Phosphoric Acid," *Ibid.*, *26*, 311–319 (1964).
30. H. Matsuoka, M. Aizawa, and S. Suzuki, "Uphill Transport of Uranium across a Liquid Membrane," *J. Membr. Sci.*, *7*, 11 (1980).
31. K. Akiba and T. Kanno, "Transport of Uranium(VI) through a SLM Containing LIX63," *Sep. Sci. Technol.*, *18*, 831–841 (1983).
32. C. N. Satterfield, C. K. Colton, and W. H. Pitcher Jr., "Restricted Diffusion in Liquids within Fine Pores," *AIChE J.*, *19*, 628 (1973).
33. L. Reikert, "The Relative Contribution of Pore Volume Diffusion and Surface Diffusion to Mass Transfer in Capillaries and Porous Media," *Ibid.*, *31*, 863 (1985).
34. H. Komiyama and J. M. Smith, "Intraparticle Mass Transport in Liquid-Filled Pores," *Ibid.*, *20*, 728 (1974).
35. R. Aris, *Ind. Eng. Chem., Fundam.*, *22*, 150 (1983).
36. C. F. Reusch and E. L. Cussler, "Selective Membrane Transport," *AIChE J.*, *19*, 736–741 (1973).
37. M. E. Duffey, D. F. Evans, and E. L. Cussler, "Simultaneous Diffusion of Ions and Pairs across Liquid Membranes," *J. Membr. Sci.*, *3*, 1–14 (1978).
38. T. Sato, "Extraction of Uranium(VI) and Thorium from Nitric Acid Solutions by TBP," *J. Appl. Chem.*, *15*, 489–495 (1965).
39. T. Sato, "The Extraction of Thorium from Nitric Acid Solutions by Di-(2-ethylhexyl) Phosphoric Acid," *J. Inorg. Nucl. Chem.*, *29*, 5563 (1967).

Received by editor January 4, 1998
Revision recieved February 1998

Request Permission or Order Reprints Instantly!